Mon. Not. R. astr. Soc. (1972) **159**, 179–190.

INTERSTELLAR CIRCULAR POLARIZATION

P. G. Martin

(Communicated by M. J. Rees)

(Received 1972 March 27)

SUMMARY

This paper shows that optical observations of circular polarization produced by aligned interstellar grains could yield valuable information about the grain material. The interstellar medium is known to be linearly dichroic from observations of interstellar linear polarization; many different grain models using a large variety of compositions can be found to reproduce these observations. Since the same aligned grains make the medium linearly birefringent, a small component of circular polarization can result from incident linearly polarized light if the position angle of the linear polarization does not coincide with either principal axis of the medium. Here calculations are presented to demonstrate that the wavelength of the circular polarization is sensitive to the imaginary part of the complex refractive index of the grain material. This provides an opportunity of investigating whether the grains are characteristically dielectric or metallic. Some possible observations are suggested.

1. INTRODUCTION

It is proposed that observations of circular (elliptical*) polarization from aligned interstellar grains could be useful in placing restrictions on the type of grain material involved. At the present many grain models based on a large variety of dielectric through metallic compositions can be found to produce a reasonable fit to the observed wavelength dependence of extinction and linear polarization in the optical region of the spectrum. However over this same range of models widely different circular polarization is predicted; thus circular polarization measurements offer a new method of resolving the longstanding ambiguity in the interpretation of existing observations. This investigation was prompted by a statement near the end of van de Hulst's monograph (1957) forseeing interstellar circular polarization; since then this interesting possibility has not received the attention it probably deserves.

In Section 2 the phenomena of dispersion and extinction in a medium containing interstellar grains and their relation to the Stokes parameters describing circular and linear polarization are reviewed. Next the wavelength dependence of circular polarization for different materials is investigated using the Mie theory for circular cylinders supplemented by the anomalous-diffraction and Rayleigh-like approximations. The circular polarization expected from some previously proposed grain materials is discussed. Finally in Section 4 several observations, including some involving non-forward scattering, are suggested.

* The term circular polarization is used to denote the circular component (Stokes parameter V) of what is generally elliptical polarization.

2. DISPERSION, EXTINCTION AND POLARIZATION

The action of interstellar grains on radiation passing through interstellar space can be shown to be equivalent to that of a medium with complex refractive index

$$\tilde{m} = \tilde{n} - i\tilde{k} = 1 - i(2\pi)^{-2}\lambda^3 NS(0) \tag{1}$$

where N is the number density of grains, λ is the wavelength of the light and $S(0)$ is the complex amplitude function of the radiation scattered in the forward direction (van de Hulst 1957); $\tilde{m}$ is close to one because N is so small. From this formal equivalence the amount of extinction and dispersion can be seen immediately. The linear extinction coefficient γ depends on the imaginary part of $\tilde{m}$;

$$\gamma = 4\pi\lambda^{-1}\tilde{k} = \pi^{-1}\lambda^2 NRe[S(0)] \equiv NC_e \tag{2}$$

where C_e is the extinction cross-section per grain. The presence of grains also produces a phase lag (or advance if ϵ is negative)

$$\epsilon = 2\pi\lambda^{-1}s(\tilde{n}-1) = (2\pi)^{-1}\lambda^2 NsIm[S(0)] \equiv \tfrac{1}{2}NsC_p \tag{3}$$

where s is the pathlength in the medium and C_p has been defined by analogy to C_e.

Both linear and circular polarization depend on interstellar grains of anisotropic shape* being aligned so that the averaged profile along the line of sight is non-circular. Observations of linear polarization are usually taken as evidence that such alignment exists, although what alignment mechanism is actually operating is not clearly understood. Except in the direction of the alignment axis of symmetry this medium has different complex refractive indices for orthogonal orientations of the electric vector of the radiation; it is convenient to choose two perpendicular directions, 1 and 2 say, along the long and short principal axes of the grain profile respectively. The symmetry is such that linear dichroism ($C_{e1} \neq C_{e2}$) and linear birefringence ($C_{p1} \neq C_{p2}$) can occur, while their circular counterparts cannot. Linear birefringence requires a non-zero imaginary part of the scattering amplitude function (a non-zero phase change). Note that linear birefringence does not necessarily imply linear dichroism (e.g. non-absorbing particles small compared to the wavelength; equations (15) and (16)) or vice-versa (Fig. 1). In addition to alignment of the grains and the resulting linear birefringence the incident radiation must be linearly polarized at a position angle other than 0° or 90° relative to the principal axes 1 and 2 for the birefringence to produce the desired circular polarization.

Changes in polarization can be described conveniently in terms of the four Stokes parameters I, Q, U, V. Here we adopt the convention that for an observer looking towards the source of radiation position angles are measured counter-clockwise from axis 2 in the plane perpendicular to the direction of propogation. Thus, for example, $V > 0$ corresponds to right-hand circular polarization in which the position angle of the electric vector increases with time (counter-clockwise rotation).

* Alignment of grains of optically anisotropic material is also possible, but is not considered in detail here.

Two useful expressions can be written down from the amplitude-phase definitions of Q and V:

$$dQ = E_2^2 - E_1^2 \simeq \tfrac{1}{2}I[(1-\gamma_2\, ds)-(1-\gamma_1\, ds)] = \tfrac{1}{2}IN\, ds(C_{e1}-C_{e2}) \quad (4)$$

$$dV = 2E_2E_1 \sin(\epsilon_2-\epsilon_1) \simeq U(\epsilon_1-\epsilon_2) = \tfrac{1}{2}N\, ds(C_{p1}-C_{p2})\, U. \quad (5)$$

These equations emphasize the following important points: that within the above convention interstellar grains produce the Q component of linear polarization, and that a component V results only when the incident radiation has a U component of linear polarization and the medium is linearly birefringent. The latter two requirements must be considered in choosing good observational prospects.

A more general treatment along the lines developed by van de Hulst (1957) and Serkowski (1962) shows that

$$I^{-1}\frac{dI}{ds} = -\tfrac{1}{2}N(C_{e1}+C_{e2})-\tfrac{1}{2}N(C_{e1}-C_{e2})(Q/I) \quad (6)$$

$$\frac{d(Q/I)}{ds} = \tfrac{1}{2}N(C_{e1}-C_{e2})-\tfrac{1}{2}N(C_{e1}-C_{e2})(Q/I)^2 \quad (7)$$

$$\frac{d(U/I)}{ds} = \tfrac{1}{2}N(C_{p1}-C_{p2})(V/I)-\tfrac{1}{2}N(C_{e1}-C_{e2})(Q/I)(U/I) \quad (8)$$

$$\frac{d(V/I)}{ds} = \tfrac{1}{2}N(C_{p1}-C_{p2})(U/I)+\tfrac{1}{2}N(C_{e1}-C_{e2})(Q/I)(V/I). \quad (9)$$

Usually only the first term on each right-hand side will be important.

Since in most observational cases the column density $N\, ds$ is not known (or is model dependent) it is useful to remove this parameter by expressing the predicted components V and Q on the same arbitrary scale and then to find the expected magnitude of V using observations of the linear polarization in that direction. (This latter step would of course give $N\, ds$ for each model if required). The ratio of equations (4) and (5) gives an indication of the size of V to be expected; if Q is 1 per cent, $C_{p1}-C_{p2} \simeq C_{e1}-C_{e2}$ and $U/I = 0{\cdot}1$ then V would be 0·1 per cent. The relative phase $\Delta\epsilon$ would be only 0·01 radians, about two orders of magnitude less than that of a quarter-wave plate.

3. WAVELENGTH DEPENDENCE OF CIRCULAR POLARIZATION

(i) *Theoretical basis*

To predict the wavelength dependence of V, it is necessary to calculate C_p on the basis of some model for the interstellar grains. As mentioned above, the size (or size distribution) can be chosen so that a match to the observed wavelength dependence of linear polarization (and extinction) is obtained. Models thus restricted show that V is sensitive to the nature of the grain material, and on this basis it is proposed that observations of V could be a useful discriminant for grain composition.

Many calculations of the linear polarization expected from aligned interstellar grains have used infinite circular cylinders as a model, since for this shape Mie solutions exist, whereas for a general spheroid no such solutions are available. Actually the Mie solutions are valid for finite cylinders of any radius as long as the conditions $l \gg a$ and $l \gg \lambda$ are satisfied (van de Hulst 1957). Microwave analogue experiments with spheroids and cylinders (Greenberg, Pederson & Pedersen 1961; Greenberg 1968) demonstrate qualitative agreement even when $l \simeq 2a$ (all wavelengths).

The Mie theory for infinite cylinders, including the case of oblique incidence, gives the cross-sections as series expansions (Lind & Greenberg 1966)

$$Q^E = \frac{C^E}{2a} = \frac{2}{x}\left(b_0{}^E + 2\sum_{n=1}^{\infty} b_n{}^E\right) \tag{10}$$

$$Q^H = \frac{C^H}{2a} = \frac{2}{x}\left(a_0{}^H + 2\sum_{n=1}^{\infty} a_n{}^H\right) \tag{11}$$

where $x = 2\pi a/\lambda$, $C = C_e + iC_p$ and the superscripts E and H identify the two polarizations with electric vectors respectively in and perpendicular to the plane formed by the cylinder axis and the direction of propagation. Both the real and imaginary parts of the complex coefficients have to be calculated when Q_s, the efficiency factor for scattering, is determined so that usually no new coefficients would have to be calculated for either Q_e or Q_p; only a regrouping of terms is necessary.

A computer program kindly supplied by N. C. Wickramasinghe was appropriately modified to include computations of Q_p. In Fig. 1 some results are shown for models chosen to match the mean observed linear polarization curve tabulated by Coyne & Gehrels (1967). No attempt is made at this point to use a size distribution

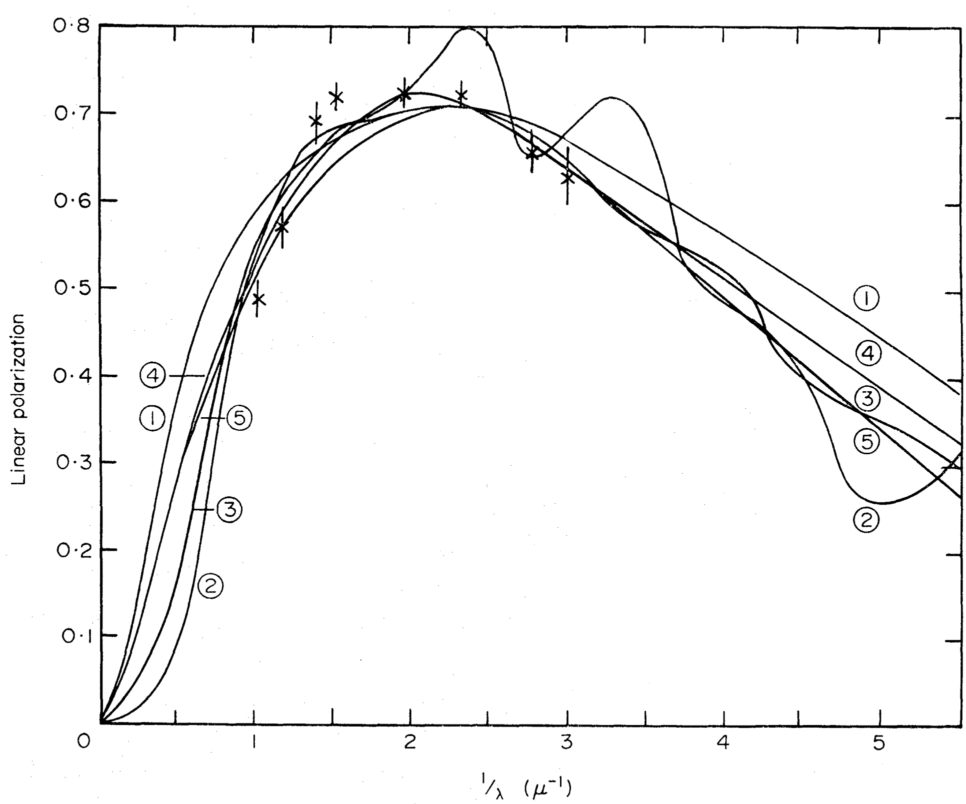

FIG. 1. *Wavelength dependence of linear polarization for different complex refractive indices ('picket fence' alignment for long circular cylinders). For each curve the vertical scale and the grain size were chosen to obtain a good approximation to the shape of the mean observed linear polarization (crosses). The vertical scale is arbitrary.* ① m = 1·1; ② m = 1·5; ③ m = 1·5–0·1i; ④ m = 1·5–0·5i; ⑤ m = 1·5–1·5i.

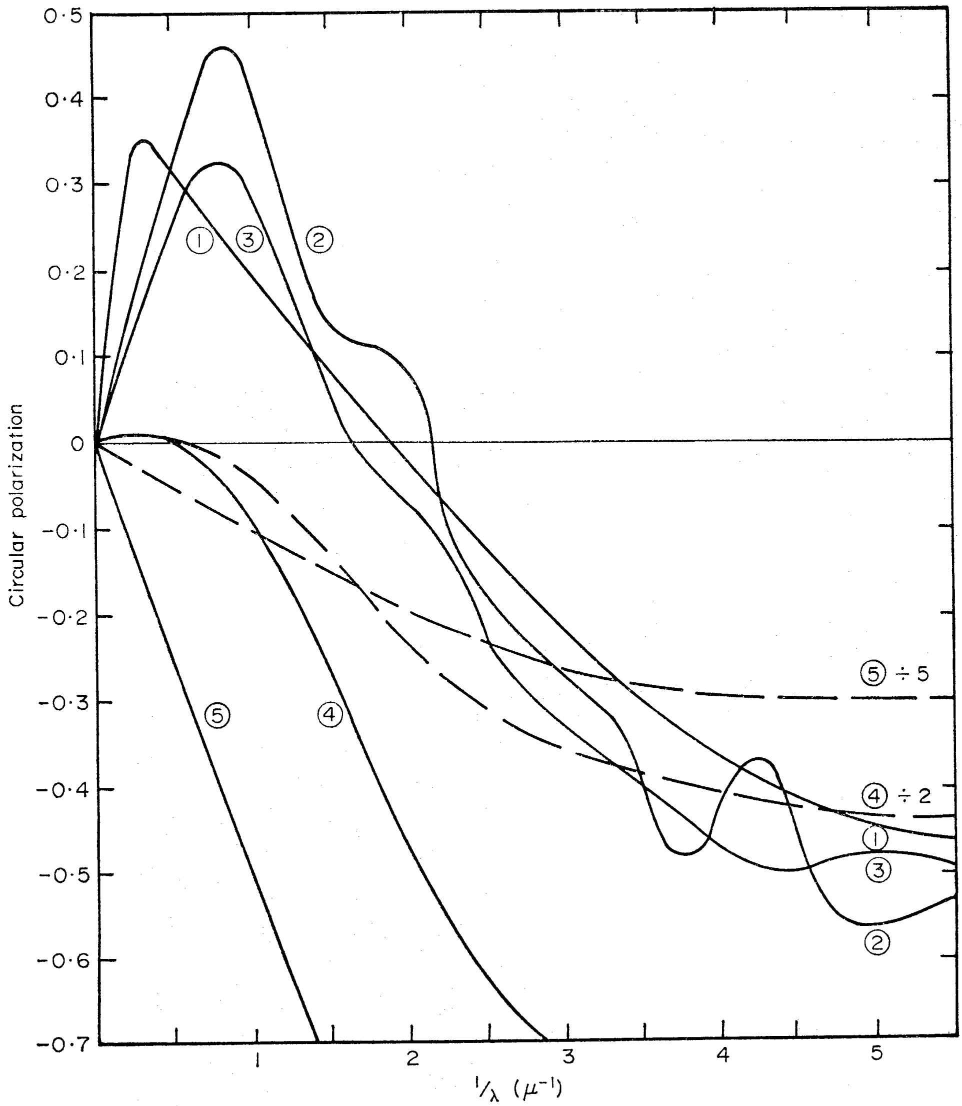

FIG. 2. *Wavelength dependence of circular polarization for the grains producing the linear polarization in Fig.* 1.

or oblique incidence since we are interested in isolating the effects of changing the complex refractive index m of the grain material. Nevertheless even for this simplified calculation for a single grain size and 'picket fence' alignment the agreement with observation is quite reasonable for each complex refractive index. (Averaging over size will smear out the oscillations in the curve(s) for $m = 1{\cdot}5$.)

What is important is that these different grains which produce similar linear polarization curves in Fig. 1 do not have the same circular polarization, as is clear from Fig. 2. Evidently changing n has little influence on the wavelength dependence of V, but it can be seen that variations in k have a large effect. Curves for the two extremes, $k = 0$ and $k \simeq n$, reveal characteristic differences. The former, for dielectric materials, have a relative phase lag at long wavelengths which reverses to an advance in the optical region. On the other hand what we shall call 'metallic' materials produce a relative phase advance which increases towards shorter wavelengths. Some insight into these different behaviours can be gained through use of approximations to the Mie theory.

(ii) *Dielectric materials*

The scalar approach of anomalous-diffraction can be used to study the dependence of Q_p on wavelength when $|m-1| \ll 1$ and $x \gg 1$. Results for perpendicular incidence (van de Hulst 1957; Cross & Latimer 1970) can be expressed in closed form as

$$Q = \pi[H_1(\rho^*) + iJ_1(\rho^*)] \tag{12}$$

where $\rho^* = 2x(m-1)$ and H_1 and J_1 are the first-order Struve function and Bessel function of the first kind respectively. In the absence of tables for complex arguments, simple numerical integrations may be performed from

$$Q = 2\int_0^{\pi/2} [1 - \exp(-\gamma \cos\alpha) \cos(\rho \cos\alpha)] \cos\alpha \, d\alpha + i2 \int_0^{\pi/2} \exp(-\gamma \cos\alpha) \sin(\rho \cos\alpha) \cos\alpha \, d\alpha \tag{13}$$

where $\rho = 2x(n-1)$. Both Q_p (upper curves) and Q_e (lower) have been plotted against ρ in Fig. 3 for $\gamma = 0$ and $\gamma/\rho = k/(n-1) = 0{\cdot}5$. It can be seen that when $\gamma \neq 0$ (dashed curve) the transmitted radiation is weakened so that its interference with the diffracted radiation is less pronounced in Q_e.

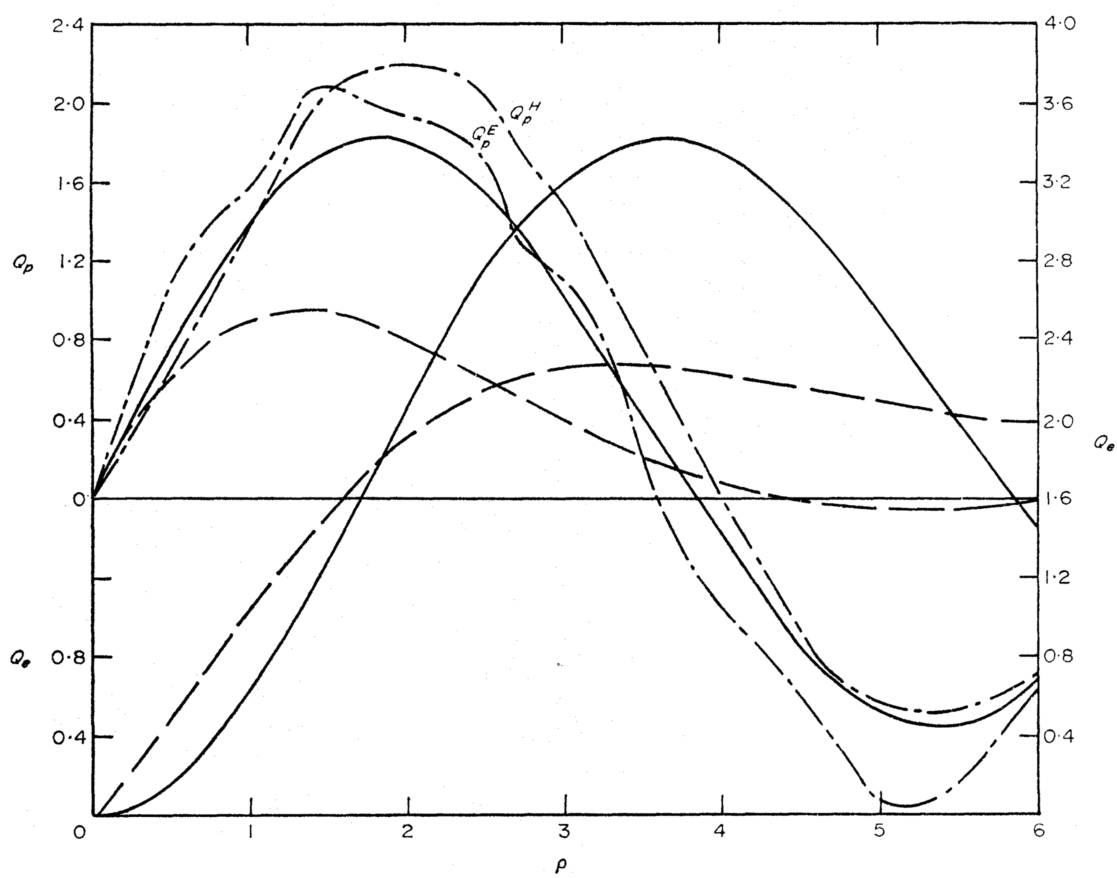

Fig. 3. *The anomalous-diffraction approximations to* Q_e (*lower*) *and* Q_p (*upper*) *at normal incidence, for two values of the imaginary part of the refractive index,* $k = 0{\cdot}0$ (*solid curves*) *and* $k/(n-1) = 0{\cdot}5$ (*dashed*). *The dashed-dotted curves show Mie theory calculations of* Q_p^E *and* Q_p^H *for* $m = 1{\cdot}5$.

The phase change Q_p represents the net effect of the grain material on the transmitted rays only. For small ρ (the central phase shift) transmitted rays passing close to the centre give the dominant contribution, so that the values of ρ for the first few extrema and zeros of Q_p are near those for the function sin ρ. However rays passing further from the centre make an increasingly significant contribution as ρ becomes larger. Absorption in the grain reduces all transmitted radiation and in particular reduces the dependence on the central radiation which suffers the most absorption. As stated by the localization principle (van de Hulst 1957) rays passing further from the centre correspond to successively higher multipoles, and from the viewpoint of the Mie theory, higher order coefficients arise from higher multipole radiation.

When m becomes much different than one the anomalous-diffraction approximation no longer holds. The curves for $Q_p{}^E$ and $Q_p{}^H$ shown for $m = 1{\cdot}5$ (dashed-dotted curves) have shapes similar to the approximate one but because the excited multipole moments for the two polarizations E and H differ (magnetic and electric multipoles respectively) the two curves are not identical. The characteristic sign change in $\Delta Q_p = Q_p{}^E - Q_p{}^H$ occurs when ρ becomes significant, since here the higher multipoles begin to be important.

It can be pointed out at this stage that application of the anomalous diffraction theory to a disk ($l \ll a$) irradiated edge-on shows that similar phenomena occur, since in fact the same formulae apply if $l \gg \lambda$; unfortunately no theory comparable to the Mie theory exists for disks when $|m-1|$ is not close to one.

In the limit of small ρ^*, to lowest order

$$Q = i\tfrac{1}{2}\pi\rho^* = i\tfrac{1}{2}\pi x 2(m-1) \tag{14}$$

in agreement with the Rayleigh–Gans results derivable for $|m-1| \ll 1$ and $|\rho^*| \ll 1$ (x arbitrary). This coincidence occurs even for $x \ll 1$ because, to this order, interference effects between the scattered radiation from neighbouring volumes of the grain do not enter.

(iii) *Metallic grains*

At this point we develop the Rayleigh-like approximation to Q ($x \ll 1$, $|m|x \ll 1$) in order to investigate the change in V as k increases. This approximation has been derived from the Mie theory for infinite cylinders ($l \gg \lambda$) by expanding the Mie coefficients in powers of x (van de Hulst 1957; Kerker, Cooke & Carlin 1970; Shah 1971). Following these results, with several simplifications to reduce Q to only terms in the first power of x, we find

$$Q^E = i\tfrac{1}{2}\pi x(m^2-1)\cos^2\theta + Q^H \sin^2\theta \tag{15}$$

$$Q^H = i\tfrac{1}{2}\pi x \frac{2(m^2-1)}{m^2+1} \tag{16}$$

where $\theta = 0$ for perpendicular incidence. When m is real there is no extinction to this order, but Q_p is not zero (linear birefringence without linear dichroism). Even though this approximation was derived with the assumption $l \gg \lambda$, to this order in x the results are identical with those from the Rayleigh approximation ($l \ll \lambda$), again because interference effects are irrelevant. Similarly for a thin disk

$$Q^{\mathrm{I}} = i\tfrac{1}{2}\pi x(m^2-1) = Q^E \tag{17}$$

$$Q^{\mathrm{II}} = i\tfrac{1}{2}\pi x\,\frac{m^2-1}{m^2}\cos^2\phi + Q^{\mathrm{I}}\sin^2\phi \tag{18}$$

where $\phi = 0$ denotes edge on incidence.

In Fig. 4 the extinction (dashed curves), and the phase shifts and circular polarization (solid curves) are shown as a function of k ($n = 1{\cdot}5$; $x = 0{\cdot}01$). Similar curves for disks are included (dash-dotted curves). The most striking feature is that at $k^2 = n^2-1$, $Q_p{}^E$ changes sign from a phase lag to an advance. On the other hand $Q_p{}^H$ is less strongly affected by increasing k because of the

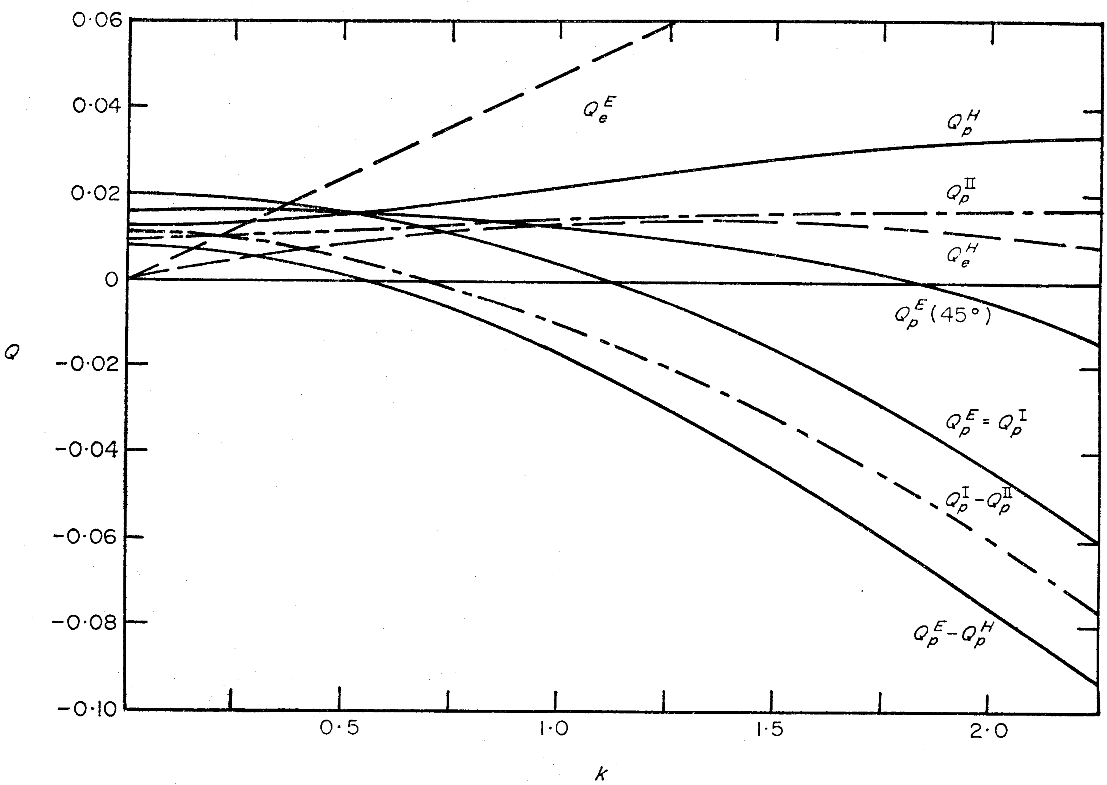

FIG. 4. *The Rayleigh approximation for* x = 0·01, n = 1·5 *and different values of* k. *Dashed curves show* Q_e^E *and* Q_e^H *for long cylinders at normal incidence and the solid curves show* Q_p^E, Q_p^H *and their difference* ΔQ_p. (Q_p^E *for* 45° *incidence is also shown*). *For disks at edge-on incidence* Q_p^{II} *and* ΔQ_p *are given by the dashed-dotted curves.*

Lorentz field, and actually remains the same sign. As a result a change of sign of $Q_p{}^E - Q_p{}^H$ occurs for $k^2 < n^2-1$. Thus for metallic grains ΔQ_p is negative; this sign persists at shorter wavelengths ($x \simeq 1$) as illustrated in Fig. 2.

For materials with complex refractive indices between these extremes the zero in ΔQ_p for dielectric grains caused by the size effect is gradually moved to longer wavelengths until it finally disappears altogether when k becomes large (Fig. 2).

(iv) *Oblique incidence and size distributions*

We consider briefly the effects of oblique incidence and a distribution of grain sizes on the above models. The wavelength dependences of both ΔQ_e and ΔQ_p are plotted in Fig. 5 for $m = 1{\cdot}5$–$0{\cdot}1i$ and $\theta = 0°$, 40° and 80° (constant size). (Curves for $m = 1{\cdot}5$ are similar but have the oscillations.) It is seen that oblique

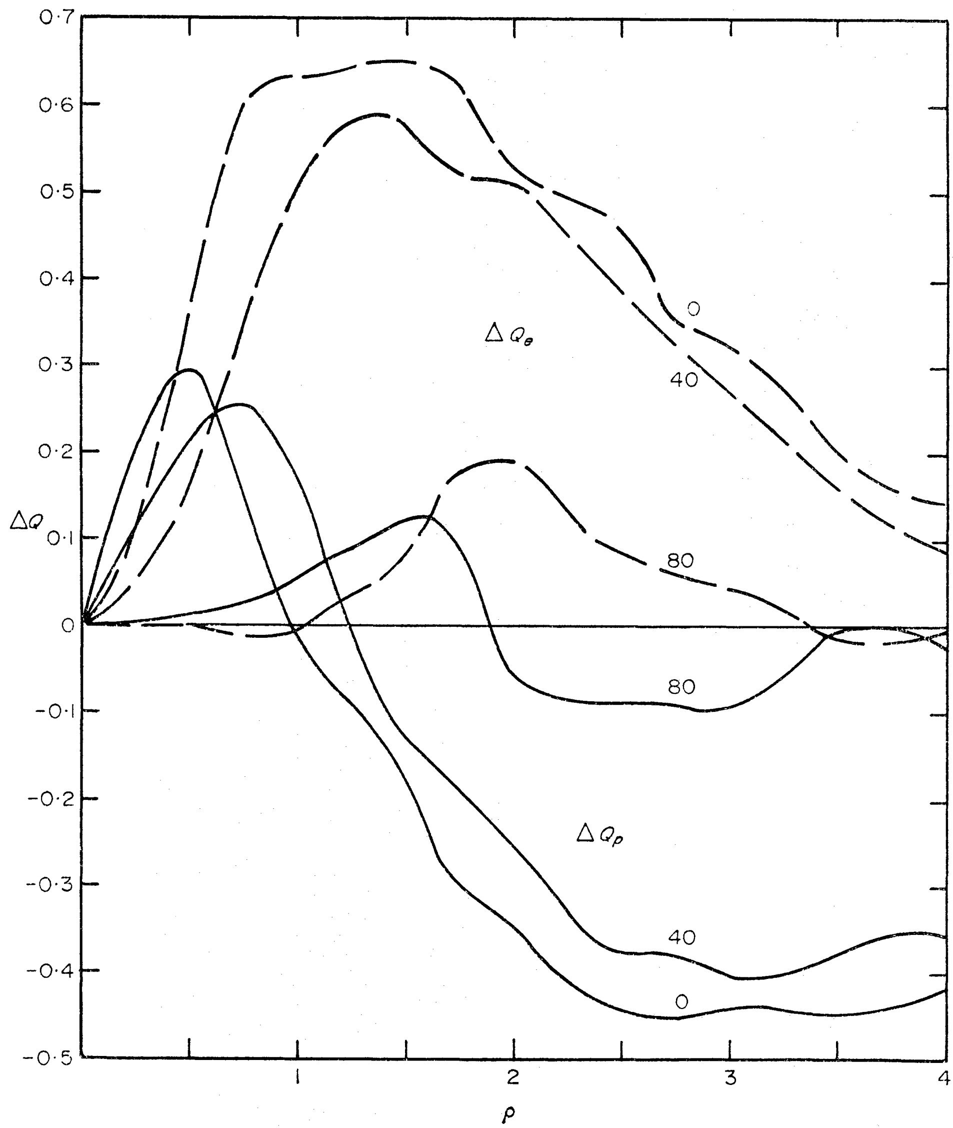

FIG. 5. *Linear and circular polarization from cylinders at perpendicular incidence* ($\theta = 0°$) *and oblique incidence* (40° *and* 80°). *Dashed curves show* ΔQ_e, *the difference in extinction efficiency factors for the two orientations of the electric vector, and solid curves show* ΔQ_p, *the corresponding difference in retardation. The complex refractive index* m = 1·5–0·1i.

incidence tends to peak the linear polarization dependence, so that better agreement with the observations is obtained. Its effect on circular polarization from dielectric grains is to reduce the amount of polarization expected in the optical region of the spectrum because the zero in ΔQ_p occurs at different wavelengths for different angles of incidence. (However the amount of linear polarization per grain also decreases.) A suitable average for realistic grain alignment can be obtained by weighting $\Delta Q_p(\theta)$ with the appropriate form of the angular distribution function (Greenberg 1968). Since changing the size of the grain also shifts the zero in ΔQ_p a size distribution will similarly reduce the optical circular polarization. The exact wavelength of the zero in ΔQ_p will depend on the size distribution, and on the detailed behaviour of the refractive index of a real grain material in the optical region of the spectrum.

The behaviour for 'metallic' grains ($m = 1·5–1·5i$) is illustrated in Fig. 6. In contrast to the more complicated situation for dielectric grains only a general

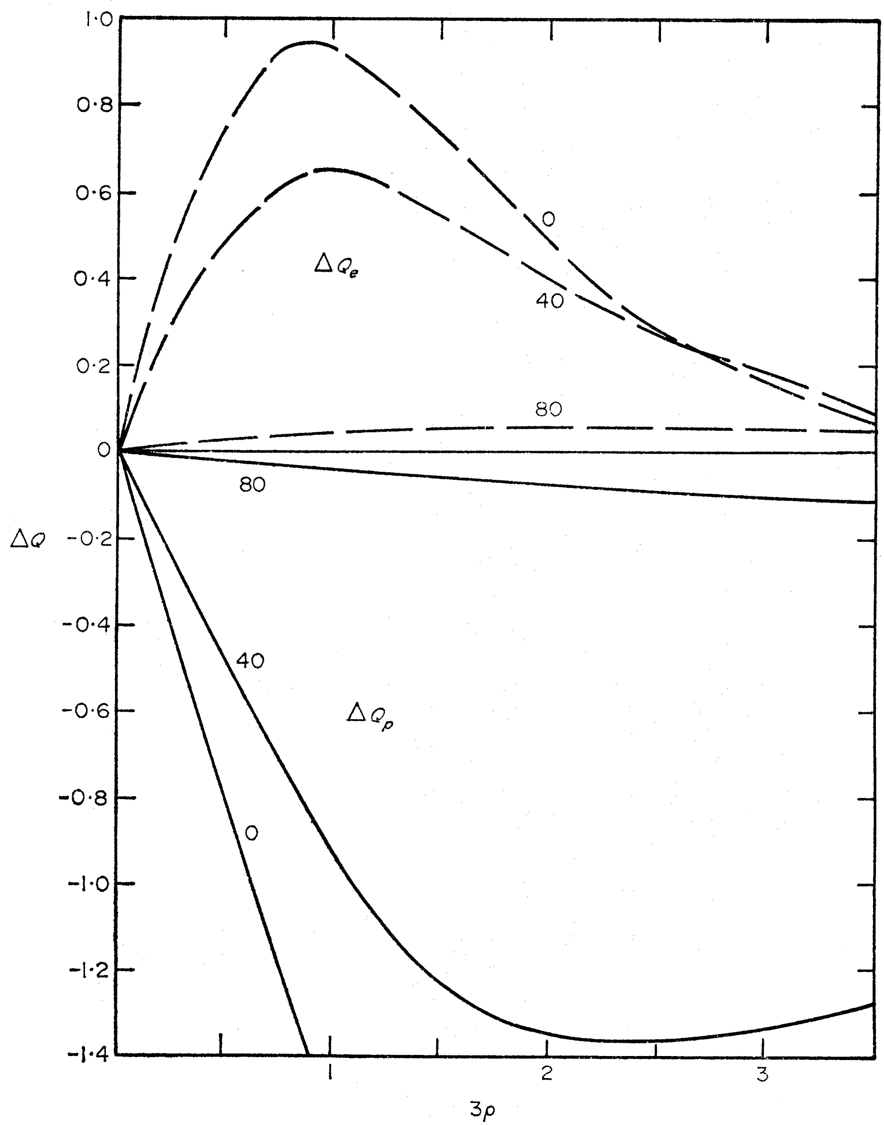

FIG. 6. *Same as Fig.* 5, *but for* m = 1·5–1·5i.

reduction of ΔQ_e and ΔQ_p occurs as the obliquity increases. Inclusion of a size distribution also will not affect the conclusion that ' metallic ' grains produce strong circular polarization in the optical region.

(v) *Circular polarization from some proposed grain materials*

Some of the materials proposed for interstellar grains are classified according to the type of circular polarization curve expected at optical wavelengths.

' Ice ', with $n \sim 1{\cdot}3$, is dielectric even when impurities raise k to 0·05 (' dirty ice ').

Silicates have $n \sim 1{\cdot}7$ with k ranging from 0 to $\sim 0{\cdot}3$. The non-absorbing variety are dielectric but those with large k would have a more ' metallic ' behaviour (Fig. 2).

Iron, with $k \sim n$ throughout the optical region, is of course metallic.

Graphite particles, which may occur in disk form (flakes), have the added complication of being optically anisotropic. When the electric vector of the incident radiation is in the plane of the flake (case I) the complex refractive index is metallic, producing a large negative Q_p^{I}. On the other hand when the electric vector is perpendicular to the flake the refractive index is dielectric, so that according to the theory of anomalous-diffraction Q_p^{II} will be positive at long wavelengths and then negative in the ultra-violet. On this basis the character of circular polarization from graphite is expected to be highly metallic.

Silicon carbide may also be present in optically anisotropic flakes. However in this case both complex refractive indices are real, the larger being $n \sim 2{\cdot}7$ for case I. Both Q_p^{I} and Q_p^{II} will have similar shapes (see Fig. 3) but Q_p^{I} will peak and cross over at longer wavelengths and have a larger amplitude because the refractive index is larger. It is expected that ΔQ_p will be dielectric in nature, having a zero near the maximum in ΔQ_e, although there might be sufficient difference to distinguish it from other dielectrics.

4. OBSERVATIONS

In conclusion we suggest some observations of V that could be made. As discussed above, observations of interstellar linear polarization can establish that the grains are aligned, the magnitude of the linear polarization Q, and the position angle relative to which the incident radiation must have a U component of polarization. It may be necessary to infer this interstellar polarization from observations of stars near the intrinsically polarized source. Sources should be chosen for which both Q (interstellar) and U are reasonably large so that V is within the range of detection. Clearly observations at a number of wavelengths would be desirable in order to make full use of the predictions of the models.

As a specific example we cite the Crab Nebula, which in addition to satisfying the above criteria offers the advantage that changes of the sign of V at different positions in the Nebula can be predicted, due to the variations in position angle that occur. In the past observations have not had sufficient accuracy to detect V, but recently some success in measuring V has been achieved. These observations are discussed in the following paper (Martin, Illing & Angel 1972).

Other possibilities include stars which show intrinsic linear polarization (late-type stars, Dyck *et al.* 1971; early-type stars, Serkowski 1970) and linearly polarized galactic nuclei, if these sources lie behind enough aligned interstellar grains. Also, as Serkowski (1962) has pointed out, if the direction of grain alignment varies strongly along the line of sight a measurable circular component could result for heavily obscured stars. From the point of view of comparing with theoretical models such observations might be of less value, because the magnitude and sign of the 'incident' polarization U are not known.

Although only forward scattering has been investigated in detail in this paper it is worth mentioning that scattering at other angles can also convert linear into elliptical polarization. This follows because, even for spheres, there are two different, generally complex amplitude functions $S(\beta)$ corresponding to different orientations of the electric vector of the incident radiation relative to the plane of scattering. These amplitude functions can be computed in a straightforward way from the appropriate Mie coefficients for forward scattering and some simple angular functions. Then the transformation of the Stokes parameters can be obtained (van de Hulst 1957). As in the case of forward scattering the phase shifts will be sensitive to the type of grain material, but in addition some knowledge of a number of other parameters such as the grain size, the angle of scattering, the space distribution of grains (some asymmetry relative to the source of illumination), and the polarization of the incident radiation or the importance of multiple scattering would be needed to construct a realistic model.

Nevertheless there are several interesting observational possibilities, such as reflection nebulae beside intrinsically polarized stars, or (asymmetric) nebulae with multiple scattering. If the light from the nucleus of M82 were linearly polarized, then observations of V in the outlying filaments might provide a method of establishing the presence of grains (Sanders & Balamore 1971).

ACKNOWLEDGMENTS

I wish to thank Professor D. A. MacRae, Department of Astronomy, University of Toronto, and Professor R. Novick, Columbia Astrophysics Laboratory, Columbia University, for their hospitality while parts of this paper were being written. This was begun during tenure of a Commonwealth Scholarship and completed with partial support by the National Science Foundation under grant GP 31356X and by the National Aeronautics and Space Administration under grant NGR 33-008-102. This is Columbia Astrophysics Laboratory Contribution No. 62.

Institute of Theoretical Astronomy, Madingley Road, Cambridge, England

and

Columbia Astrophysics Laboratory, Columbia University, New York, New York 10027

REFERENCES

Coyne, G. & Gehrels, T., 1967. *Astr. J.*, **72**, 892.
Cross, D. A. & Latimer, P., 1970. *J. opt. Soc. Am.*, **60**, 904.
Dyck, H. M., Forrest, W. J., Gillett, F. C., Stein, W. A., Gehrz, R. D. & Woolf, N. J., 1971. *Astrophys. J.*, **165**, 57.
Greenberg, J. M., 1968. *Stars and Stellar Systems*, **7**, 221, eds B. M. Middlehurst and L. H. Aller, University of Chicago Press.
Greenberg, J. M., Pedersen, N. E. & Pedersen, J. C., 1961. *J. appl. Phys.*, **32**, 233.
Kerker, M., Cooke, D. D. & Carlin, J. M., 1970. *J. opt. Soc. Am.*, **60**, 1236.
Lind, A. C. & Greenberg, J. M., 1966. *J. appl. Phys.*, **37**, 3195.
Martin, P. G., Illing, R. & Angel, J. R. P., 1972. *Mon. Not. R. astr. Soc.*, **159**, 191.
Sanders, R. H. & Balamore, D. S., 1971. *Astrophys. J.*, **166**, 7.
Serkowski, K., 1962. *Adv. Astr. Astrophys.*, **1**, 290.
Serkowski, K., 1970. *Astrophys. J.*, **160**, 1083.
Shah, G. A., 1971. *Nature, Phys. Sci.*, **232**, 184.
Van de Hulst, H. C., 1957. *Light Scattering by Small Particles*, Wiley, New York.